EFFECTS OF FLAPPING WING MICRO AIR VEHICLE'S PITCHING ANGLE ON STABILITY AT LOW REYNOLDS NUMBER

Mohamed Mowhoub [1] **and Ermira Junita Abdullah** [1,*]

1. Department of Aerospace Engineering, Faculty of Engineering, Universiti Putra Malaysia, 43400 Serdang, Selangor, Malaysia

*Correspondence: ermira@upm.edu.my

Abstract: The instability of flapping wing aircraft makes them difficult to control. As it is challenging to control and puts passengers at risk, it is not currently employed in modern aircraft technology. This study aims to analyze the aerodynamic coefficients of flapping wing aircraft at different flapping angles in order to understand their effects on the aircraft's stability. XFLR5 software was used to calculate the aerodynamics coefficients and longitudinal derivatives in different range of flapping angles from 40° to -40°. This range of flapping angles has been selected for the purpose of this study based on the physical limitations of a mechanical vehicle. Theoretically, an aircraft without a tail is unstable because the main function of a tail is to produce a moment that counters the moment produced by the wings to balance the aircraft. In the presented research, a model has been designed with and without tail, and modeled using XFLR5 to produce the aerodynamics coefficients. Then, MATLAB software was used to develop the longitudinal flight dynamics for the model. The results show that the longitudinal motion is stable for the range of flapping angle between 40° to -40°. The natural frequency increases as flapping angle changes from 0° to 40° and from 0° to -40°. In the meantime, for the short period mode's eigenvalue, the real part moves toward the origin as the flapping angle changes from 0° to 40° and from 0° to -40°. On the other hand, for the phugoid mode's eigenvalue, the real part moves away from the origin to the left half plane as the flapping angle changes from 0° to 40° and from 0° to -40°.

Keywords: flapping wing; MAV; aerodynamic coefficients; stability; flight dynamics

1. Introduction

In general, the aerospace industry is always evolving through implementation of new technologies into old and existing ones. It can be noted that the foundation of the industry is largely based on nature creatures such as birds, insects and others [1]. The flapping wing aircraft is an example of the earliest technologies that mankind has tried to make or replicate from nature. However, due to the complexities and challenges, flapping wing aircraft was not used and several other types of inventions such as fixed wing aircraft has been used instead because their efficiency [2]-[5]. Flapping wing aircraft is essentially difficult to develop because of inconsistency in terms of its stability. It is not implemented in today's aircraft technology due to limited understanding of its dynamics. With better understanding, an optimal controller can be developed to produce a safe flapping wing flight. To this effect, there are conducted researches that have demonstrated the benefits of using flapping wing, though implementation of such methods might be more suitable for the smaller-size micro air vehicles (MAVs) [6]-[11].

For flapping wing aircraft to find wider applications in the aerospace industry, such as for passenger transport missions, more studies are required to better understand its flight dynamics. With this notion, the research work presented in this paper is aimed to analyze the aerodynamic coefficients of flapping wing aircraft at different flapping angles. The knowledge gained from this study helps to establish their

influence on the aircraft's stability and subsequently facilitates the design of a better controller for a safe flapping wing flight.

2. Methodology

In XFLR5 software, a flapping wing model was created based on the work by Bomphrey et al. [2]. The model was updated with Phoenix airfoil for the main wing section and NACA 0009 airfoil for the tail section. Once airfoils were specified and analyzed, the creation of the new plane model in XFLR5 was completed. It should be noted that the NACA 0009 airfoil was chosen since it is symmetrical and commonly recommended for the aircraft's tail section [12]. Figure 1 illustrates the isometric view of the designed plane model in XFRL5 and Table 1 lists the parameters of the model.
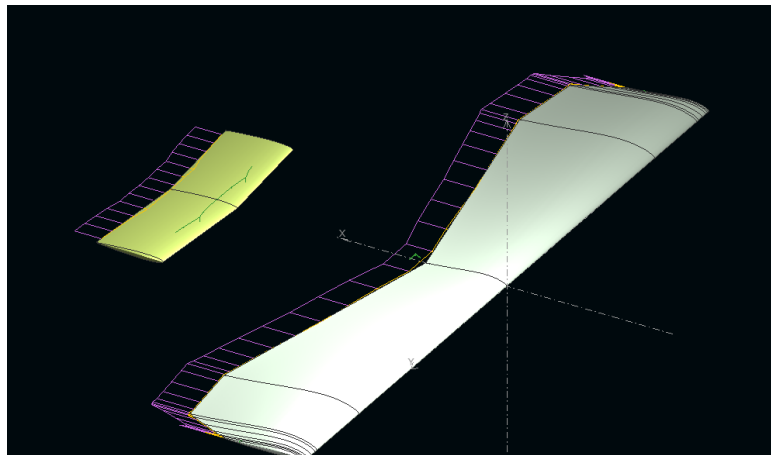

Figure 1: Isometric view of the designed plane model in XFLR5

Table 1: Parameters of model from XFLR5

Parameter	Value
wingspan	1.56 m
xyProj. Span	1.56 m
Wing Area	0.39 m^2
xyProj. Area	0.39 m^2
Plane Mass	2.25 kg
Wing Load	5766.048 g/m^2
Tail Volume	0.445
Root Chord	0.18 m
MAC	0.256 m
Tip Twist	0
Aspect Ratio	6.237
Taper Ratio	1
Root-Tip Sweep	0
XNP = d($XC_p.C_l$)/dc_l	0.112 m

Firstly, using XFLR5 software, aerodynamics and stability analyses were done on the entire model to obtain its aerodynamics coefficients at Reynolds number of 6×10^6. Using the obtained aerodynamic coefficients and also previously estimated model parameters, the stability coefficients were computed. In this study, MATLAB software is applied in the calculation of the longitudinal and lateral coefficients

based on formulas from Nelson [13]. Next, the stability derivatives were calculated. Subsequently, the corresponding state matrix, natural frequency and damping ratio were derived. These parameters were then utilized to simulate the plane model.

2.1. Equations of longitudinal motion

A first-order vector differential equation known as the state equation describes the natural form of aircraft motion. It is a mathematical representation of the aircraft's stability and control. The following Equation 1 describes the current condition of a trimmed aircraft, where A is the state coefficient matrix, $\vec{x}$ is the state vector, B is the driving matrix and $\vec{u}$ is the control vector [13].

$$\dot{x} = A\vec{x} + B\vec{u} \tag{1}$$

Moreover, the longitudinal state equation is given by the following Equation 2.

$$\begin{bmatrix} \dot{u} \\ \dot{w} \\ \dot{q} \\ \dot{\theta} \end{bmatrix} = \begin{bmatrix} X_u & X_w & 0 & -g \\ Z_u & Z_w & U_o & 0 \\ M_u & M_w & M_q & 0 \\ 0 & 0 & 1 & 0 \end{bmatrix} \begin{bmatrix} u \\ w \\ q \\ \theta \end{bmatrix} + \begin{bmatrix} X_\eta \\ Z_\eta \\ M_\eta \\ 0 \end{bmatrix} \eta \tag{2}$$

To use this state equation, the coefficients are first needed to find the longitudinal derivatives [12]. In general, the longitudinal derivatives can be attributed to changes in forward speed, pitching velocity and also time rate of change of angle of attack. Firstly, changes in the aircraft's forward speed will also alter its drag, lift and pitching moments. Plus, the aircraft's thrust is also a function of its forward speed. Meanwhile, the derivatives due to pitching velocity correspond to the change in the z-force and pitching moment coefficients caused by the pitching velocity, which is represented by stability coefficients, C_{zq} and C_{mq}. The aircraft's pitching motion affects the aerodynamic properties of both wing and horizontal tail. In most cases, the wing contribution pales in comparison to that of the tail. On the other hand, the derivatives due to time rate of change of angle of attack relate to the lag in wing's downwash reaching the tail section and causing the stability coefficients below to increase. The circulation around the wing will change as its angle of attack varies. The downwash at the tail is altered by the change in circulation. However, the change takes a finite amount of time to occur. All in all, after calculating the coefficients, the longitudinal derivatives can be derived and the longitudinal state equation is obtained [13].

2.2. Validation study

In order to show that the steps and process followed in this study were correct, an initial case study was conducted for validation purposes. This validation study was made based on the presented case of Cessna 172 aircraft wing that was published by Hidayat et al. [14]. The wing model, which has NACA 2412 airfoil cross-sectional shape, was constructed in XFLR5 and it is as shown in Figure 2. The wing model was then analysed in XFLR5 under the same analysis settings as those specified in the reference literature. In this case, the Mach number was set to 0.19 and the range of Reynolds number was between 6×10^6 to 6.5×10^6, with increment of 500,000.

The analysis results from XFLR5 in the form of the plot of lift coefficient versus angle of attack is presented in Figure 3(a) while the one from the published reference is depicted in Figure 3(b). It can be observed that the two results are essentially consistent and greatly in line with each other, which is taken to validate the adequacy of steps and process used in this study. With this notion, the same methodology was applied in the analysis of the designed plane model that was the main focus of this study.
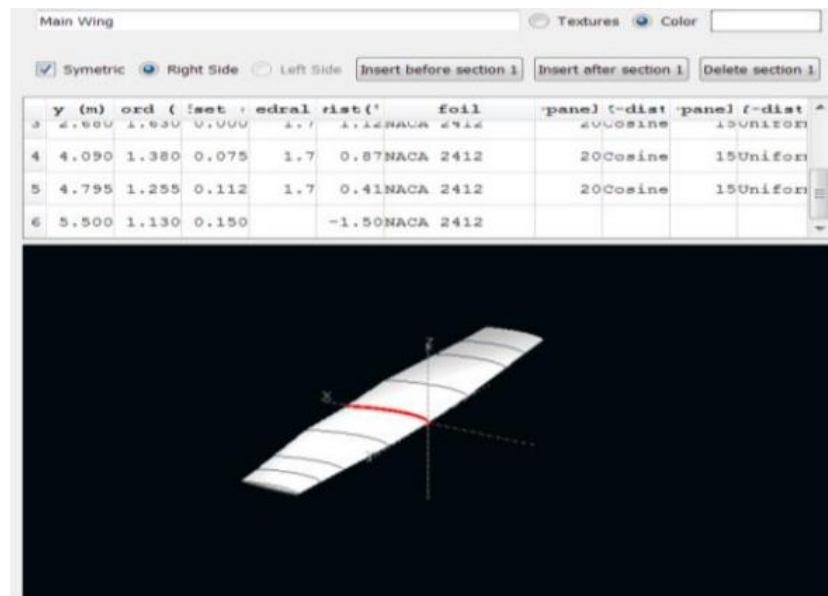
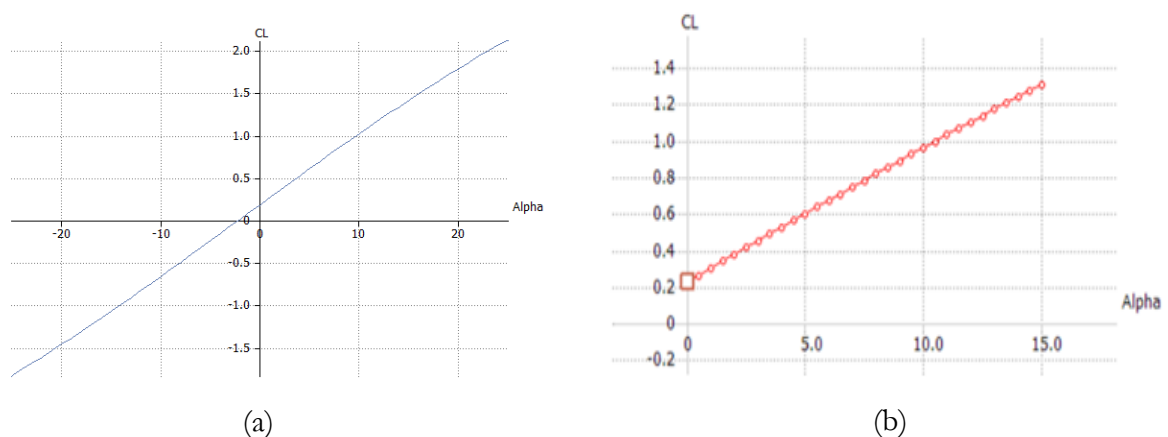Figure 2: Constructed Cessna 172 aircraft wing model based on the study by Hidayat et al. [14]

| (a) | (b) |

Figure 3: Plot of lift coefficient versus angle of attack from: (a) validation study in XFLR5, (b) reference literature by Hidayat et al. [14]

3. Results and Discussion

Figure 4 shows the airfoil analysis results for both the Phoenix and NACA 0009 airfoils from the XFLR5 software. In this figure, the result for Phoenix airfoil is marked by red color whereas those for the NACA 0009 airfoil is indicated by blue color. Figure 4(a) depicts plot of lift coefficient, C_l versus angle of attack, α. It essentially shows how these two airfoils behave in three main regions: linear, non-linear and post stall regions. As can be observed, value of C_l initially increases linearly with increment in α. However, at some point, C_l starts to decrease with further increase of α until it reaches the stall region, where the value of C_l decreases drastically. At this stall region, the wing has more pressure on its upper surface than its lower surface. For the Phoenix airfoil, it starts losing lift and enters stall region at $\alpha = 11°$. At the same angle of attack, referring to Figure 4(b), it can be seen that the drag coefficient, C_d increases exponentially, which results in higher drag and decrease in the ratio of C_l/C_d as presented in Figure 4(c). Similar observations can be made with regard to the results for NACA 0009 airfoil, which appears to stall at lower angle of attack than that for the Phoenix airfoil.
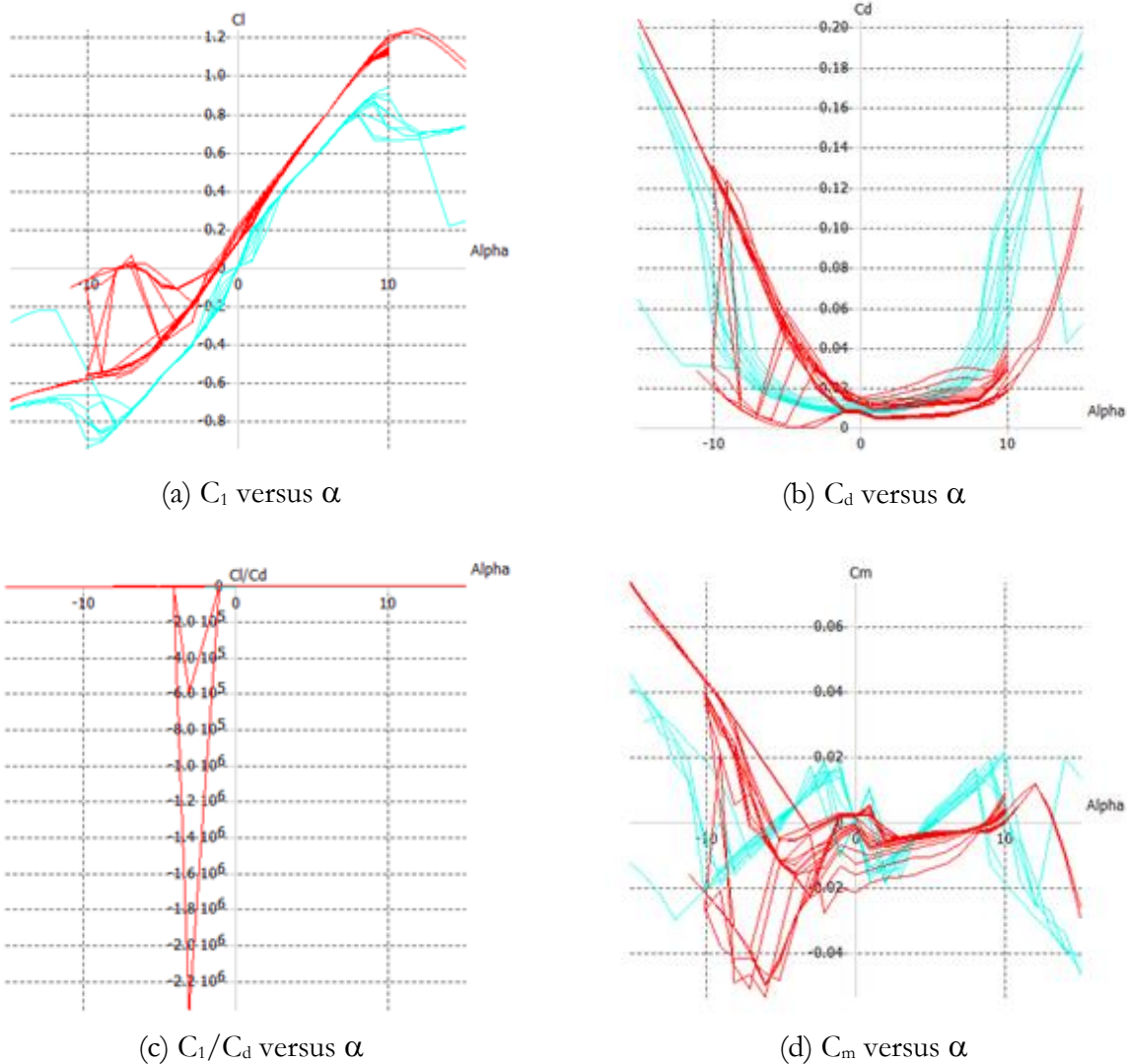
(a) C_l versus α

(b) C_d versus α

(c) C_l/C_d versus α

(d) C_m versus α

Figure 4: Airfoil analysis results for Phoenix airfoil (red) and NACA 0009 airfoil (blue)

On the other hand, the analysis results from XFLR5 on the designed model are presented in Figure 5. Of particular interest in terms of stability is the plot of the moment coefficient, C_M versus α that is shown in Figure 5(d). It can be observed that the slope of this C_M versus α plot is positive, which means that the plane model fulfills the longitudinal static stability criterion and can be trimmed. However, the plane cannot be trimmed at positive angles of attack and this condition is reflected by the negative value of angle of attack where the line plot intercepts the α-axis. Meanwhile, looking at Figure 5(c) that depicts the plot of C_L/C_D versus α, the value of C_L/C_D starts to decrease after $\alpha = 5°$ and this implies that plane is maybe close to entering its stall region where drag increases and lift decreases. Using the aerodynamics data obtained from XFRL5, the longitudinal coefficients were calculated using MATLAB. For flapping angle of 0°, the calculated values are tabulated in Table 2. These coefficients were then applied to obtain the dynamics model, natural frequency, damping ratio and eigenvalues. Finally, with this information, the stability of the model could be determined.

For longitudinal dynamics, the eigenvalues are found to be -5.5233 + 34.9633i, -5.5233 – 34.9633i, -0.0285 + 0.2335i, and -0.0285 – 0.2335i. It can be observed that the eigenvalues are complex and the real parts of the root are negative. This indicates that the system is dynamically stable, which means that if the system was given an initial disturbance, the motion would be sinusoidal but would not grow with time and therefore it is considered to be stable. The natural frequency for the short period and phugoid

mode were found to be 35.3969 and 0.2352, respectively. In the meantime, damping ratios for the short period and phugoid mode were found to be 0.1560 and 0.1210, respectively.

(a) C_L versus α

(b) $C_{D\_viscous}$ versus α

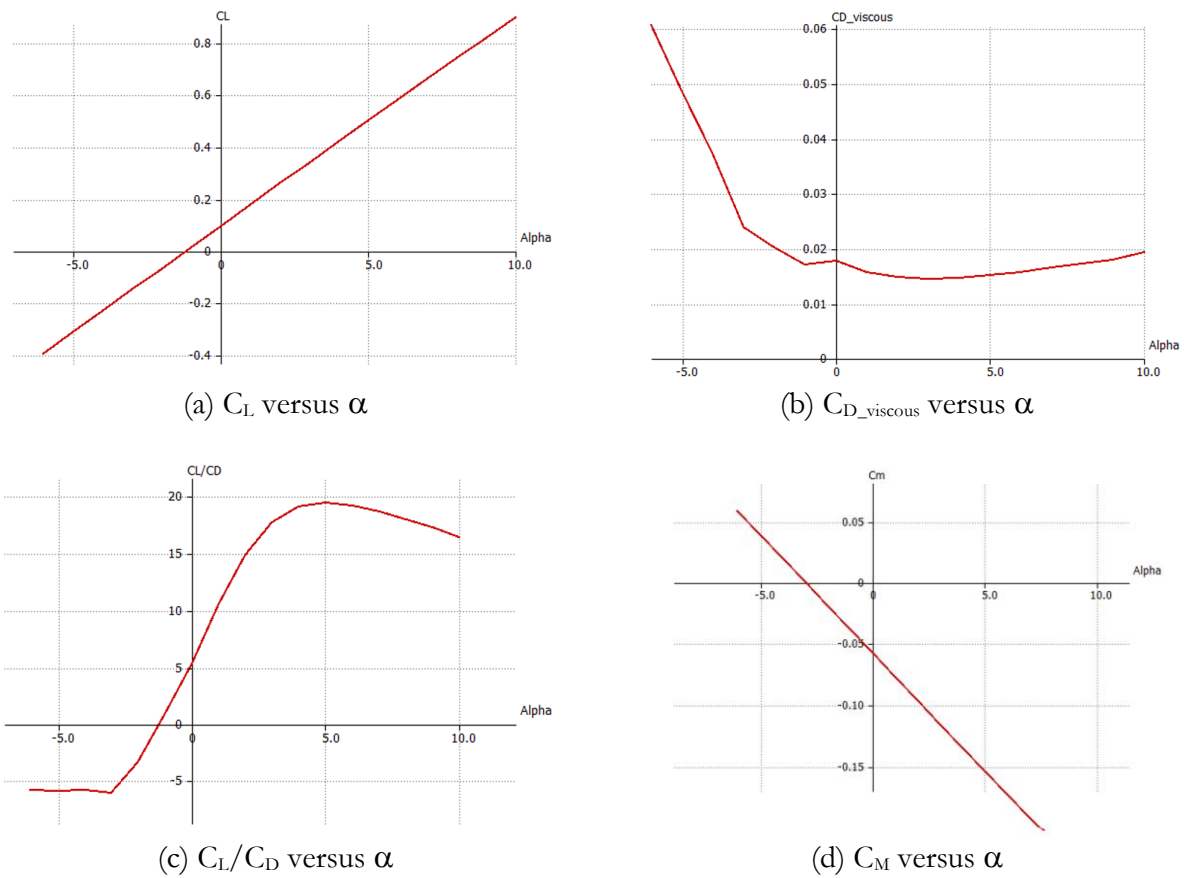(c) C_L/C_D versus α

(d) C_M versus α

Figure 5: Aerodynamics analysis results of the designed plane model

Table 2: Longitudinal coefficients at flapping angle of 0° as obtained from MATLAB

Stability Coefficients	Value
C_{x_u}	-0.0540
C_{x_a}	0.0543
C_{z_u}	-0.1440
C_{z_α}	-4.6680
$C_{z_{\dot{\alpha}}}$	-1.3491
C_{z_q}	-2.8437
$C_{z_{\delta_e}}$	-0.2427
C_{m_a}	-2.5456
$C_{m_{\dot{\alpha}}}$	-3.1619
C_{m_q}	-6.6650
$C_{m\delta_e}$	-0.5688

Moreover, Figure 6 presents the summary for the longitudinal motion at 0° pitching. The first plot in Figure 6(a) shows the behavior of forward speed, u versus time, t. It shows that the amplitude of u is decreasing as time increases. In this case, the amplitude decreases to -40 in 10 seconds, which might indicate that aircraft is not generally stable in terms of forward speed. This situation might be because the plane model does not have a propulsive system since it is a glider and changes in thrust is expected. Meanwhile Figure 6(b) shows the change of vertical speed, w with time, t. The plot indicates that the amplitude of w oscillates between 0 and -0.4 at the start for roughly less than 1 second before becoming stable with minimum change in amplitude. In the meantime, Figure 6(c) shows the plot of pitch change, q versus time, t. It can be observed from the plot that the amplitude of q becomes constant after nearly half a second. Its amplitude appears to oscillate between 2 to -6 at the beginning and then decease to 0. Lastly, the final plot in Figure 6(d) shows the change in pitch angle, α against time, t. It can be seen in the plot that the change in amplitude of α is very small, which ranges between 0 to -0.4. Furthermore, the amplitude oscillates between -0.2 to -0.4 in about 8 seconds, which is considered very stable.
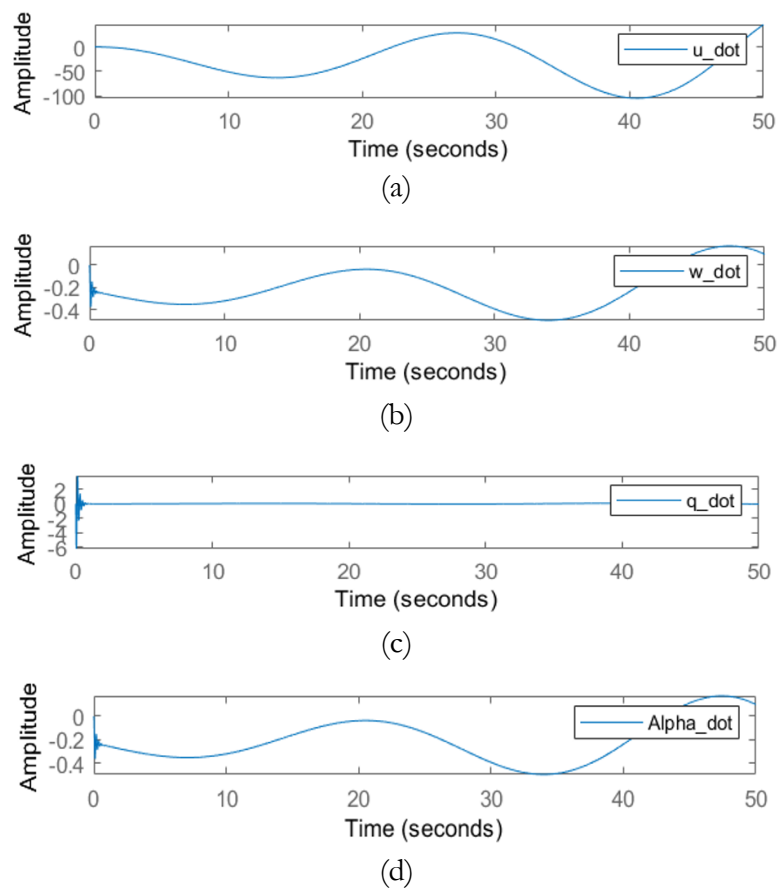

(a)

(b)

(c)

(d)

Figure 6: Longitudinal response for pitching angle of 0°

The same analysis was repeated for other flapping angles from -40° to 40° and the comparison of obtained results in terms of the natural frequency in longitudinal long period mode is shown in Figure 7. It can be observed that the highest frequency of about 35 rad/sec was recorded at 0° angle while the lowest frequency of 21 rad/sec was recorded at both 40° and -40° angles. In general, it can be seen that as the flapping angle increases, the natural frequency decreases. On the other hand, Figure 8 shows the comparison of natural frequency for short period mode at different flapping angles. In short, the angles of 0°, 10° and 20° appear to have the same frequency of 0.235 rad/sec while all other angles have higher frequency with maximum of 0.266 rad/sec for flapping angles of 40° and -40°. Subsequently, essentially similar observations for the comparison of damping ratios at different flapping angles were obtained as

illustrated by Figure 9 and Figure 10. Furthermore, Table 3 tabulates the corresponding longitudinal eigenvalues for long and short period modes. It can be seen that all of the eigenvalues have a positive real root, which indicates that the aircraft is stable. Additionally, as flapping angle moves further from 0°, the eigenvalues come closer to the origin point, which is 0.
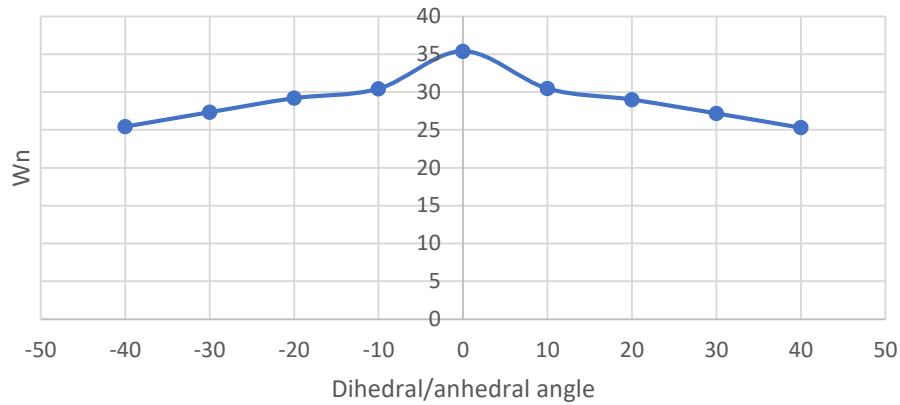

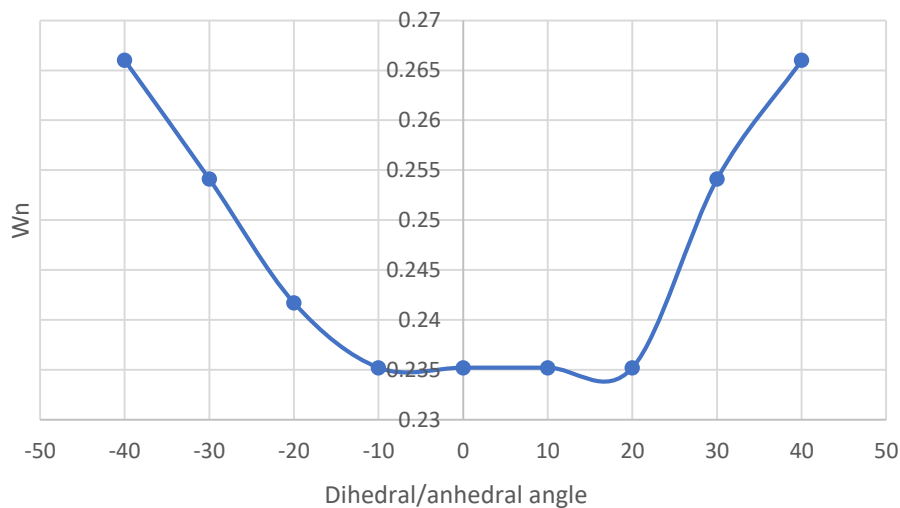Figure 7: Natural frequency comparison for longitudinal long period

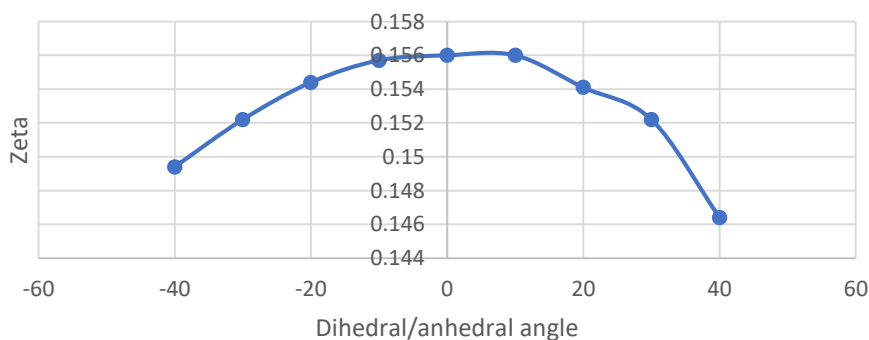Figure 8: Natural frequency comparison for longitudinal short period

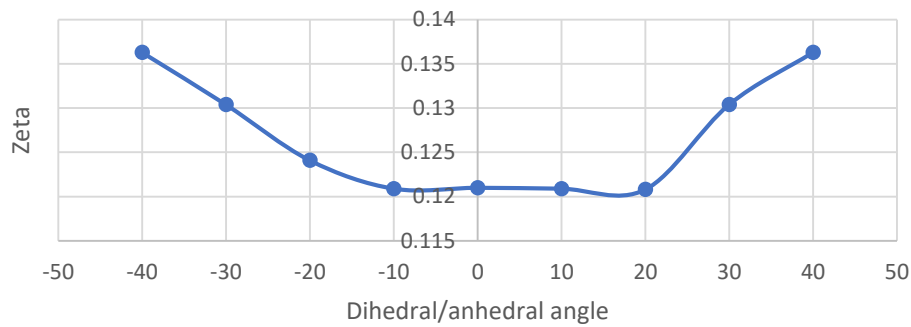Figure 9: Damping ratio comparison for longitudinal long period

Figure 10: Damping ratio comparison for longitudinal short period

Table 3: Longitudinal eigenvalues for all considered flapping angles

Angle (°)	Mode	Eigenvalues
40	Short period	-3.7795 ± 25.1072i
	Phugoid	-0.0363 ± 0.2635i
30	Short period	-4.1378 ± 26.8753i
	Phugoid	-0.0331 ± 0.252i
20	Short period	-4.4718 ± 28.6654i
	Phugoid	-0.0284 ± 0.2335i
10	Short period	-4.7547 ± 30.1062i
	Phugoid	-0.0284 ± 0.2335i
0	Short period	-5.5233 ± 34.9633i
	Phugoid	-0.0285 ± 0.2335i
-10	Short period	-4.741 ± 30.0785i
	Phugoid	-0.0284 ± 0.2335i
-20	Short period	-4.5081 ± 28.8478i
	Phugoid	-0.03 ± 0.2398i
-30	Short period	-4.1629 ± 27.0252i
	Phugoid	-0.0331 ± 0.0252i
-40	Short period	-3.8021 ± 25.1573i
	Phugoid	-0.0363 ± 0.2635i

4. Conclusion

In this study, a model of flapping wing plane has been constructed using Phoenix and NACA 0009 airfoils as the cross-sectional shape of the main wing and tail sections, respectively. This flapping wing vehicle's model requires the tail section to provide balance as the main function of this tail section is to produce a moment that counters the moment that is produced by the main wing section. Based on the conducted stability analysis, it was demonstrated that this model could perform well for flapping wing vehicles. The results show that the longitudinal motion is stable for the range of flapping angle between 40° to -40°. The natural frequency is shown to increase as the flapping angle increases from 0° to 40° and -40°. For the short period mode's eigenvalue, the real part moves towards the origin as the flapping angle increases from 0° to 40° and -40°. On the other hand, for the phugoid mode's eigenvalue, the real part is shown to move away from the origin to the left half plane as the flapping angle is increased

from 0° to 40° and -40°. The subsequent future work can be done on evaluating the dynamics stability of the flapping wing model at a lower Reynolds number in the range of 10^4 to 10^5. The sizing and shape of the airfoils can also be explored to find the optimal design for use in MAVs at low Reynolds number. This will provide designers with more understanding and a range of suitable options in designing MAVs.

References

[1] N. Slosar, 'Avians to Airplanes: Biomimicry in Flight and Wing Design', Berkeley Scientific Journal, vol. 25. No. 2, pp. 25-27, 2021.

[2] R. J. Bomphrey, T. Nakata, P. Henningsson and H. T. Lin, 'Flight of the Dragonflies and Damselflies', Philosophical Transactions of the Royal Society B: Biological Sciences, vol. 371, no. 1704, 20150389, 2016.

[3] M. F. Platzer, K. D. Jones, J. Young and J. C. S. Lai, 'Flapping Wing Aerodynamics: Progress and Challenges', AIAA Journal, vol. 46, no. 9, pp. 2136-2149, 2008.

[4] R. H. Siddique, Y. J. Donie, G. Gomard, S. Yalamanchili, T. Merdzhanova, U. Lemmer and H. Hölscher, 'Bioinspired Phase-separated Disordered Nanostructures for Thin Photovoltaic Absorbers', Science Advances, vol. 3, no. 10, e1700232, 2017.

[5] F. Mazhar and S. I. Ali Shah, 'On the Unsteady Aerodynamics and Design of Flapping Wing Vehicles', International Bhurban Conference on Applied Sciences and Technology, Islamabad, Pakistan, 14-18 January, 2020.

[6] C. P. Du, J. X. Xu and Y. Zheng, 'Modeling and Control of a Dragonfly-like Micro Aerial Vehicle', Advances in Robotics and Automation, vol. S2, no. 2, 006, 2015.

[7] J. Chahl, N. Chitsaz, B. McIvor, T. Ogunwa, J. Kok, T. McIntyre and E. Abdullah. 'Biomimetic Drones Inspired by Dragonflies Will Require a Systems Based Approach and Insights from Biology', Drones, vol. 5, no. 2, 24, 2021.

[8] M. Hassanalian, G. Throneberry and A. Abdelkefi, 'Investigation on the Planform and Kinematic Optimization of Bio-inspired Nano Air Vehicles for Hovering Applications', Meccanica, vol. 53, pp. 2273-2286, 2018.

[9] T. Ogunwa, B. McIvor, N. Awang Jumat, E. Abdullah and J. Chahl, 'Longitudinal Actuated Abdomen Control for Energy Efficient Flight of Insects', Energies, vol. 13, no. 20, 5480, 2020.

[10] B. Liang and M. Sun, 'Dynamic Flight Stability of a Hovering Model Dragonfly', Journal of Theoretical Biology, vol. 348, pp. 100-112, 2014.

[11] N. Marimuthu, E. J. Abdullah, D. L. A. Majid and F. I. Romli, 'Conceptual Design of Flapping Wing Using Shape Memory Alloy Actuator for Micro Unmanned Aerial Vehicle', Applied Mechanics and Materials, vol. 629, pp. 152-157, 2014.

[12] M. S. Sarker, S. Panday, M. Rasel, M. A. Salam, K. M. Faisal and T. H. Farabi, 'Detail Design of Empennage of an Unmanned Aerial Vehicle', AIP Conference Proceedings, vol. 1919, no. 1, 020033, 2017.

[13] R. C. Nelson, Flight Stability and Automatic Control, WCB/McGraw Hill, 1998.

[14] F. T. Hidayat, B. Rabeta, F. F. Prodi, "Analisis Pengaruh Winglet Pada Sayap Pesawat Cessna 172 Menggunakan Perangkat Lunak XFLR5', Jurnal Teknologi Kedirgantaraan, vol. 5, no. 1, pp. 48–54, 2020.